Applied Surface Science 256 (2010) 6279–6283

Contents lists available at ScienceDirect

Applied Surface Science

journal homepage: www.elsevier.com/locate/apsusc

Microscale steps and micro–nano combined structures by anodizing aluminum

G.Q. Ding[a,b], R. Yang[a,b], J.N. Ding[a,b,*], N.Y. Yuan[a,b], W.Z. Shen[c]

[a] Center for Low-Dimensional Materials, Micro–Nano Devices and System, Jiangsu Polytechnic University, 1 Ge Hu Road, Changzhou 213164, Jiangsu, China
[b] Key Laboratory of New Energy Source, Changzhou 213164, China
[c] Department of Physics, Shanghai Jiao Tong University, 1954 Hua Shan Road, Shanghai 200030, China

ARTICLE INFO

Article history:
Received 19 January 2010
Received in revised form 1 April 2010
Accepted 1 April 2010
Available online 8 April 2010

PACS:
62.23.St
81.16.Rf
82.45.Yz
81.16.Dn

Keywords:
Microstep
Nanopore
Anodic alumina
Assembly
Pitting

ABSTRACT

In this paper, we firstly present a novel microscale-step structure fabricated by anodizing aluminum in a mixture of 0.05–0.5 wt% NaCl (HCl), 2 wt% H_3PO_4 and 20 wt% ethanol under potentials of 1–40 V at room temperature. Then, we present two micro–nano combined structures by integrating the microsteps with nanopores through multi-step anodizations. The microstep–nanopore hierarchical structure was obtained by re-anodizing the sample in oxalic acid, and the regular nanopores can be realized on the microscale patterned aluminum surface. The two-layer porous structure was one layer of nanoporous anodic alumina and another layer of micropores by two-step anodization on sample's both sides. These two novel structures can be useful for surface engineering and high flux filtration, respectively. The current fabrication approach broadens the applications of aluminum anodization, and brings a new method for assembling micro–nano structures.

1. Introduction

As a nanoscale template, porous anodic alumina (PAA) membranes are versatile for fabrication and assembly of nanostructured materials since PAAs have 2D nanopores with controllable pore structure, interpore distance (D_{int}) and thickness by adjusting electrolyte compositions, temperature, anodizing potentials and durations [1–3], as shown in the sketch map of Fig. 1(a). The pore structures and D_{int} will directly influence all PAAs' applications [4–6]. In addition to the general circular pores, new pore structures, such as triangle, square, diamond, nanotubes and periodic porous sheets, have been fabricated to broaden PAAs' applications. Diamond and hybrid triangle-diamond pore structures were realized by coating a polymethylmethacrylate layer and pre-patterning diamond structures on aluminum surface with electron-beam lithography [7]. Highly ordered square [8] and triangle [9] nanopore arrays in anodic alumina are obtained by oil pressing the aluminum surface with a SiC molds which have an array of convex features. Well-defined nanoporous alumina membrane sheets and novel three-dimensional (3D) nanostructures were obtained through pulse anodizations [10]. Alumina nanotubes can be realized by similar pulse anodization [11] or chemical erosion [12]. The ordered alumina nanotips [13], nanowires [14] and nanowalls [15] were also realized through various technical approaches. In summary, the well-known two-step anodization process only brings circular alumina nanopores, and additional steps, such as pre-texturing and post-treatments, are essential for other pore structures.

Besides the pore structure, the control on the D_{int} of PAAs is also very important. Masuda et al. [16] employed Fe_2O_3 monodisperse nanoparticles as a template to leave a concave array on aluminum surface to obtain PAA with D_{int} of 13 nm. Li et al. [17] reported well-ordered PAAs with D_{int} from 50 to 420 nm in three typical electrolytes. Perfectly ordered PAA with 490 nm D_{int} was realized by imprinting the aluminum foil twice with a straight-line diffraction gating and anodizing in diluted H_3PO_4 under 195 V for 1 h at 5 °C [18]. The reported largest D_{int} is 1.2 μm under ultrahigh anodizing potential of 620 V at −10 °C in the mixture of 0.3 M oxalic acid and ethanol [19]. As we know, the D_{int} is linearly dependent on the applied potential with a proportional constant 2.0–2. 5 nm V^{-1}. In order to get microscale pores, high potential (>500 V) is needed, and the destructive burning effect easily happens under such high potential. So very low temperature and ethanol were employed to dissipate the heat and avoid burning.

* Corresponding author at: Center for Low-Dimensional Materials, Micro–Nano Devices and System, Jiangsu Polytechnic University, 1 Ge Hu Road, Changzhou 213164, Jiangsu, China. Fax: +86 519 86330095.
E-mail addresses: gqding@gmail.com (G.Q. Ding), dingjn@jpu.edu.cn (J.N. Ding).

0169-4332/$ – see front matter © 2010 Elsevier B.V. All rights reserved.
doi:10.1016/j.apsusc.2010.04.004

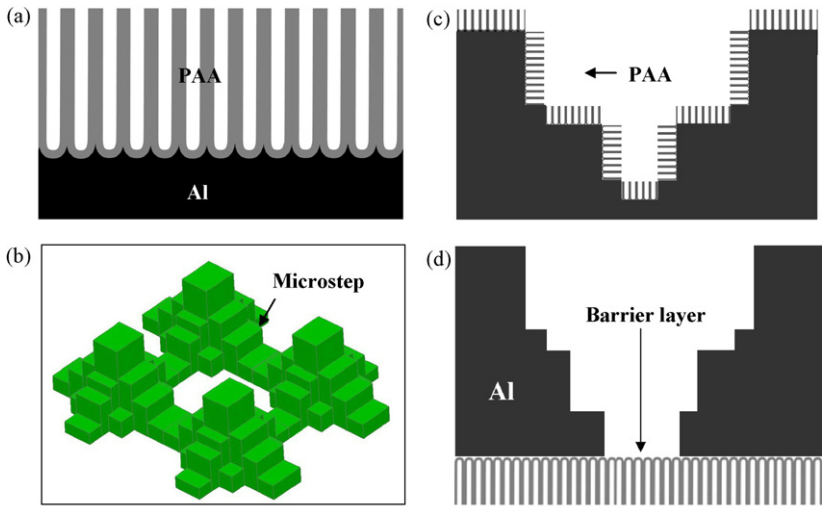

Fig. 1. Sketch maps of (a) PAA with nanopores, (b) micropores surrounded by microsteps, (c) micropore–nanopore hierarchical and (d) two-layer structures.

Here, for the first time, we report a brand-new microstep structure on aluminum surface, which is obtained through a simple one-step anodizing process at room temperature and low potential (1–40 V) in Cl^- containing electrolyte. The microsteps can self-arrange into micropores, as shown in the 3D sketch map of Fig. 1(b). Furthermore, two novel structures were integrated from microsteps and nanopores. One novel hierarchical structure was obtained by further anodizing the sample in oxalic acid to form nanopores, as demonstrated in Fig. 1(c). Another novel two-layer structure was fabricated by anodizing the sample from another side until the current density decreased significantly, as shown in Fig. 1(d). The hierarchical structure can be used for surface engineering, such as adjusting wettability and friction, and the two-layer structure can be applied for high flux filtration.

2. Experimental details

Aluminum foil (99.999%) was degreased in acetone, and then washed with deionized water. The micropores were fabricated in a mixture of 0.05–0.5 wt% NaCl (HCl), 2 wt% H_3PO_4 and 20 wt% ethanol under potentials of 1–40 V and room temperature. The sample was thoroughly washed and secondly anodized in 0.3 M oxalic acid under 40 V for 5–30 min at 20–50 °C to obtain microstep–nanopore hierarchical structure, and the third anodization could be conducted to improve the regularity of nanopores. Two-layer structure was obtained by firstly anodizing in 0.3 M oxalic acid under 40 V at 30 °C for 1–30 min and secondly anodizing in Cl^- containing electrolyte for various durations. The anodization process is monitored by Keithley 2400 source meter, and the sample morphology was characterized by field emission scanning electric microscope (FESEM, Philips XL30FEG with a spatial resolution of 2 nm). The Contact angles (CAs) of water were measured by Krüss drop shape analysis system 100 at room temperature with 3 μL water drip on five independent points.

3. Results and discussion

Fig. 2(a) and (b) shows the typical surface morphology of the fabricated microsteps. The average width, length and height of the steps are 0.5–2, 1–5 and 1–3 μm, respectively. The microsteps are not as ordered as the ideal structure as shown in the sketch map in Fig. 1(b), but they do have some regulations of their arrangement. They are basically perpendicular to each other, and their spatial dimensions are of same order of magnitude. It is these regulations that make this new, interesting and useful microporous structure happen on aluminum surface. The formation mechanism of these microsteps and micropores should be similar to the pitting process since they are both obtained in Cl^- containing electrolytes [20–26]. But pitting process, which is characterized by lower anodizing potentials (<1 V) in the electrolytes containing NaCl, HCl or $HClO_4$, only happens on some spots, and then grows deeper and deeper into the bulk aluminum to form some random holes on surface, while our microsteps can cover most of the sample surface by optimizing the anodizing conditions, especially the electrolyte composition (phosphoric acid and ethanol) and applied potentials. The formation mechanism of microsteps may also relate to the applied external stress since they were found on highly stressed aluminum under 23 V in 20 wt% sulfuric acid without any Cl^- ions [27].

We have tried various conditions to fabricate these microsteps, especially the pre-treatment (electrochemical polishing), applied potentials (1–40 V) and Cl^- concentrations (0.05–0.5 M). It is well known that the electrochemical polishing can remove a thin layer of surface aluminum, which has microscale rolling patterns, and bring ultra-flat surface with height fluctuation less than 20 nm [28,29]. But we found that the anodization on electropolished samples brought fewer microsteps and tended to be pitting process. Higher voltage (>10 V) was helpful for forming more micropores, and if the voltage was lower than 1 V, the anodization was close to the pitting process although the ethanol and phosphoric acid were added. More Cl^- dramatically increased the current density under the same potential, but decreased the amounts of microsteps. The replacement of HCl to NaCl will not affect the micropores' morphology. Energy dispersive X-ray spectrum on these microsteps confirms that the main component is aluminum with small amount of chloride. It is notable that although the potential is less than 40 V, the growth rate of the micropores layer can be as high as 3–20 μm/min while that of the general PAA layer is just ~0.05 μm/min by mild anodization. Generally, lower Cl^- concentration (0.05–0.1 M) and higher potential (10–40 V) are suitable for microstep fabrication without electropolishing.

Fig. 2(c) shows the surface morphology after re-anodizing microsteps in 0.3 M oxalic acid under 40 V at 50 °C for 5 min. It is clear that the nanopores form on the surface of microsteps, and that the straight-line edges of microsteps are remained after nanopores' formation. In order to improve the regularity of nanopores, the samples were immersed into a mixture of 6.0 wt% H_3PO_4 and 1.8 wt% H_2CrO_4 at 60 °C for 60 min to remove the oxide layers, and then anodized for the third time to get a new PAA layer, as shown in Fig. 2(d) and (e). It is interesting that most right-

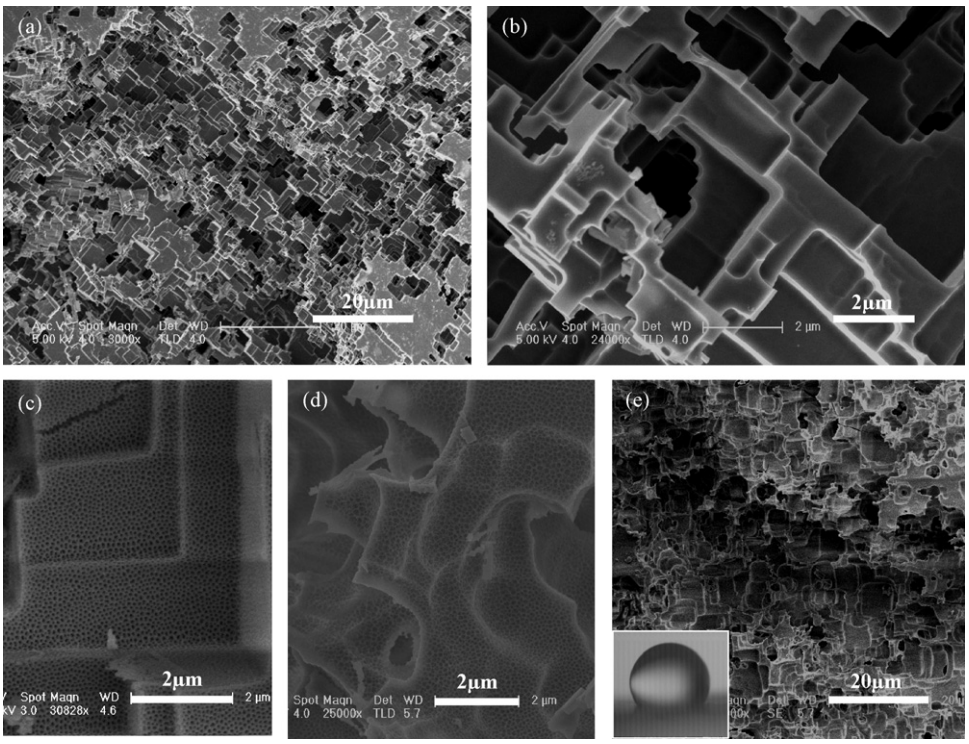

Fig. 2. FESEM images of (a) and (b) micropores with different magnifications obtained in a mixture of 0.5 wt% NaCl, 2 wt% H_3PO_4 and 20 wt% ethanol under 2 V and room temperature for 5 min, and combined microstep–nanopore hierarchical structure after second (c) and third (d) anodization in 0.3 M oxalic acid under 40 V at 50 °C for 5 min after first anodization in a mixture of 0.2 wt% NaCl, 2 wt% H_3PO_4 and 20 wt% ethanol under 9 V and 30 °C for 10 min, (e) low magnification image of (d) with the inset of the CA test result.

angled parts and those straight-line edges disappear, and that arcs come into being, which can be explained as that during the second anodization, the outstanding positions will cause stronger electric field distribution and were anodized faster than other parts. So after removing the PAA layer and anodizing for the third time, there were only arc-like parts left, as shown in the larger area image of Fig. 2(e). Fig. 2(c)–(e) confirms that the combined microstep–nanopore hierarchical structure is successfully realized by simple two- or three-step electrochemical methods.

It is well known that aluminum surface is critical for the formation of ordered nanopores of PAAs. That is why electrochemical polishing is conducted before the anodization [28,29]. Whether PAAs can form on the microscale surface fluctuation was studied by observing the sample's cross sections. Fig. 3(a)–(c) shows the cross-sections of the PAA layers after anodization in 0.3 M oxalic acid under 40 V and 50 °C for 5 min. All of them can verify that the basic microstructure of PAA layer on the microstep has no difference with that of generally reported PAA layer on flat aluminum surface. Furthermore, we reveal vivid morphology about the PAA formation on complicated surfaces, such as the arc-like surface and the connecting parts of the flat and arc in Fig. 3(b), and cone-like aluminum ends in Fig. 3(c). There do have a little differentiation from common PAAs, such as the special barrier type along the white line in Fig. 3(b) and different thickness at different parts in Fig. 3(c).

All the FESEM images in Figs. 2 and 3 confirm the formation of micropores and the successful integration of microsteps and nanopores. This obtained microstep–nanopore hierarchical structure actually is a bionic design, and it is similar to the superhydrophobic nanobranch-on-micropapillae leaf structure of lotus and rice [16]. CA test shows that this hierarchical structure is hydrophobic with the water CA ~ 140°, while the bulk alumina is hydrophilic with CA ~ 60°. More interestingly, we obtained

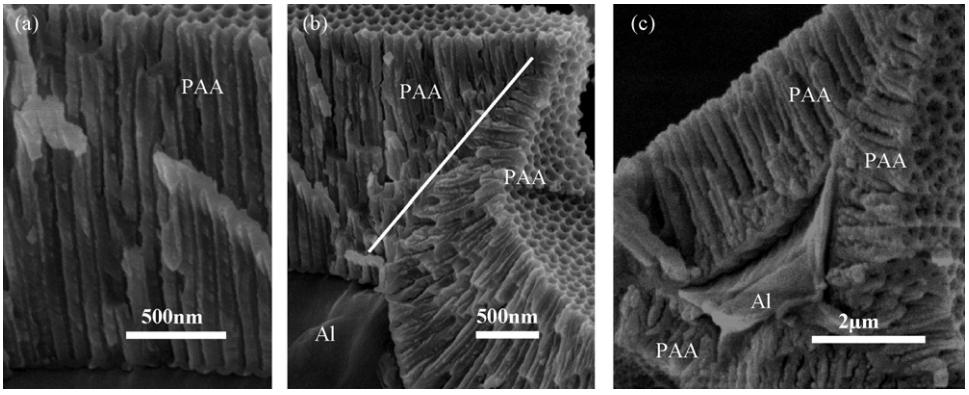

Fig. 3. (a)–(c) The cross-sectional FESEM images showing the PAA formation on microsteps, which was fabricated by first anodization in a mixture of 0.5 wt% NaCl, 2 wt% H_3PO_4 and 20 wt% ethanol under 1 V and 30 °C for 5 min on one side and second anodization in 0.3 M oxalic acid under 40 V at 50 °C for 5 min on the other side.

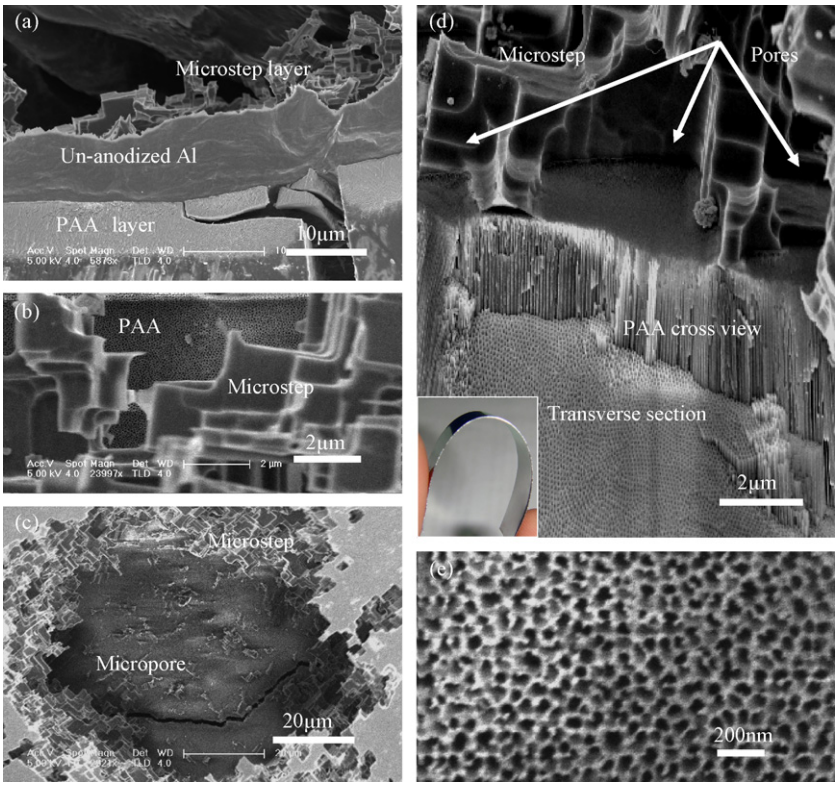

Fig. 4. FESEM images of (a) three-layer structure with partial un-anodized aluminum in the middle, the sample was firstly anodized in 0.3 M oxalic acid under 40 V and 30 °C for 20 min and secondly anodized in 0.05 wt% NaCl, 2 wt% H_3PO_4 and 20 wt% ethanol under 5 V and 30 °C for 20 min, (b) combined two-layer structure by further anodizing the sample under the same conditions for 20 min, the PAA's barrier layer was removed in 5 wt% H_3PO_4 under 30 °C for 40 min, large micropores (c) and the cross-sectional view (d) of the two-layer structure by over time anodization (total time 104 min in Cl^- containing electrolyte), (e) top view of PAA layer with throughout pore, the PAA's barrier layer was removed in 5 wt% H_3PO_4 under 30 °C for 5 min.

microstep–nanowire structure by partially dissolving the wall of nanopores to form nanowires in 5 wt% phosphoric acid at 30 °C. CA test presented a unique superhydrophilic behavior that a water drop disappeared in less than 0.2 s after it contacted with the sample surface. So, it is possible to develop a controllable wettability switch based on the capability to modify the PAA surface to nanowires [30], nanotips [13] and larger pores [19], and the capability to further optimize the micropore structure.

Another micro–nano structure, the novel two-layer structure, was obtained by two separate anodizations on the both sides of aluminum foil. To well control the thickness of PAA layer, anodize the sample in 0.3 M oxalic acid under 40 V at first, and conduct second anodization in Cl^- containing electrolyte on the other side. Fig. 4(a) shows a three-layer structure: top micropores, middle continuous un-anodized aluminum and bottom nanopores. The middle layer will disappear as the micropores grow and reach the PAA layer (Fig. 4(b)), which can be monitored by a sudden and continuous drop in the anodizing current. The 3D micropores can grow up as more and more aluminum is consumed, and large micropore with the diameter ~20 μm can be formed as shown in Fig. 2(c). The microsteps, nanopores and micropores, as well as their arrangement, are well demonstrated in the cross-sectional view at the interface of two layers in Fig. 4(d). Before this two-layer structure is used for filtration, the barrier layer of PAA needs to be removed. One way is to directly put the sample into 5% H_3PO_4 to dissolve the half-sphere cap, and the other way is to minimize the thickness of PAA barrier layer by stepwise decreasing the applied potential and then opening the nanopores in acid for very short time. Fig. 4(e) shows the morphology of the throughout PAA after opening the nanopore by lowering the potential to 5 V and chemically erosion in 5% H_3PO_4 for 5 min.

The combined two-layer structure can be utilized for high selective and high flux filter. High selectivity is due to highly order nanopore array with very low standard deviation in pore diameter, and high flux can be realized by minimizing the thickness of nanopore layer. The commercial PAA filters from Whatman™ generally has a thickness of ~100 μm, and even thicker since thin PAA film itself is too brittle to handle [31,32]. However, we can well control the PAA layer with the thickness from just 100 nm to several microns according to our research [33], and this thin PAA layer can be well bonded to the thicker (can be more than 200 μm) aluminum microstep layer. Besides the selectivity and flux, another outstanding performance of this two-layer structure is that when the PAA layer is just 100–1000 nm, the sample has very good toughness as shown in the inset picture of Fig. 4(d). It is easy to understand that the microstep layer has good toughness because aluminum is so soft. The PAA layer can also be soft when its thickness goes down to less than 1000 nm, which is consistent with our observation that in the deionized water, the ultrathin free-standing PAA will easily roll into column by itself before transferring it onto the other substrates. Compared to the commercialized PAAs, the current two-layer filter has the advantages: (1) high selectivity since its regularity is better than commercial one; (2) high flux due to its much thinner PAA layer; (3) better toughness; (4) less manufacture time due to very fast microstep fabrication and very short time for the much thinner PAA layer.

4. Conclusions

In summary, we realized microsteps on aluminum with a speed ~3–10 μm/min by anodization in a mixture of 0.05–0.5 wt% NaCl (HCl), 2 wt% H_3PO_4 and 20 wt% ethanol under potentials of

1–40 V and room temperature. The micropores are surrounded by microsteps, and the width, length and height of those steps are all in microscale, which makes the 3D micropores come into being. Furthermore, we successfully integrate these microsteps with nanopores to get two novel structures. The microstep–nanopore hierarchical structure was obtained through further anodization in 0.3 M oxalic acid on same surface, and the wettability of this structure could be superhydrophobic and superhydropholic depending on surface modification of the PAA layer. The two-layer porous structure was fabricated by controllable two-step anodization at both sides of aluminum foil, and can be used for high selective and flux filtration.

Acknowledgments

This work was supported by New Century Excellent Talents (NCET-04-0515), Qing Lan Project (2008-04), Key Programs for Science and Technology Development of Jiangsu (BE20080030) and Changzhou Science and Technology Platform (CM2008301).

References

[1] W. Lee, R. Ji, U. Gösele, K. Nielsch, Nat. Mater. 5 (2006) 741.
[2] Y. Li, Z.Y. Ling, S.S. Chen, J.C. Wang, Nanotechnology 19 (2008) 225604.
[3] G.D. Sulka, W.J. Stepniowski, Electrochim. Acta 54 (2009) 3683.
[4] H. Chik, J.M. Xu, Mater. Sci. Eng. R. 43 (2004) 103.
[5] Y. Lei, W. Cai, G. Wilde, Prog. Mater. Sci. 52 (2007) 465.
[6] Y.Z. Piao, H.C. Lim, J.Y. Chang, W.Y. Lee, H. Kim, Electrochim. Acta 50 (2005) 2997.
[7] J.T. Smith, Q.L. Hang, A.D. Franklin, D. Janes, T.D. Sands, Appl. Phys. Lett. 93 (2008) 043108.
[8] H. Asoh, S. Ono, T. Hirose, M. Nakao, H. Masuda, Electrochim. Acta 48 (2003) 3171.
[9] H. Masuda, H. Asoh, M. Watanabe, K. Nishio, M. Nakao, T. Tamamura, Adv. Mater. 3 (2001) 189.
[10] W. Lee, K. Schwirn, M. Steinhart, E. Pippel, R. Scholz, U. Gösele, Nat. Nanotechnol. 3 (2008) 234.
[11] W. Lee, R. Scholz, U. Gösele, Nano Lett. 8 (2008) 2155.
[12] Z.L. Xiao, C.Y. Han, U. Welp, H.H. Wang, W.K. Kwok, G.A. Willing, J.M. Hiller, R.E. Cook, D.J. Miller, G.W. Crabtree, Nano Lett. 2 (2002) 1293.
[13] Q.W. Sun, G.Q. Ding, Y.B. Li, M.J. Zheng, W.Z. Shen, Nanotechnology 18 (2007) 215304.
[14] Y.T. Tian, G.W. Meng, T. Gao, S.H. Sun, T. Xie, X.S. Peng, C.H. Ye, L.D. Zhang, Nanotechnology 15 (2004) 189.
[15] X.X. Sun, J. Jiang, J.F. Zhao, Q. Ma, B.S. Xu, Appl. Phys. A 98 (2010) 263.
[16] H. Masuda, Y. Matsui, K. Nishio, Small 2 (2006) 522.
[17] A.P. Li, F. Müller, A. Birner, K. Nielsch, U. Gösele, J. Appl. Phys. 84 (1998) 6023.
[18] Z.Y. Fan, H. Razavi, J.W. Do, A.M. Moriwaki, O. Ergen, Y.L. Chueh, P.W. Leu, J.C. Ho, T. Takahashi, L.A. Reichertz, S. Neale, K. Yu, M. Wu, J.W. Ager, A. Javey, Nat. Mater. 8 (2009) 648.
[19] Y. Li, Z.Y. Ling, S.S. Chen, X. Hu, X.H. He, Chem. Commun. 46 (2010) 309.
[20] M.A. Amin, Electrochim. Acta 54 (2009) 1857.
[21] S. Ono, T. Makina, R.S. Alwitt, J. Elctrochem. Soc. 152 (2005) B39.
[22] A. Despić, V.P. Parkhutik, in: J.O. Bockris, R.E. White, B.E. Conway (Eds.), Modern Aspects of Electrochemistry, Plenum, New York, 1989, p. 401.
[23] T. Martin, K.R. Hebert, J. Electrochem. Soc. 148 (2001) B101.
[24] C.S. Chi, Y. Jeong, S.S. Kim, J.H. Lee, H.J. Oh, Mater. Sci. Forum 475–479 (2005) 385.
[25] K. Nishio, T. Fukushima, H. Masuda, Electrochem. Solid-State Lett. 9 (2006) B39.
[26] M.R. Song, L. Song, S.L. Xu, Z.J. Zhang, Electrochim. Acta 53 (2008) 7198.
[27] G.D. Sulka, S. Stroobants, V.V. Moshchalkov, G. Borghs, J.P. Celis, J. Electrochem. Soc. 151 (2004) B260.
[28] A. Rauf, M. Mehmood, M.A. Rasheed, M. Aslam, J. Solid-State Electromchem. 13 (2009) 321.
[29] V.V. Konovalov, G. Zangari, R.M. Metzger, Chem. Mater. 11 (1999) 1949.
[30] Z.H. Yuan, H. Huang, S.S. Fan, Adv. Mater. 14 (2002) 303.
[31] I. Vlassiouk, A. Krasnoslobodtsev, S. Smirnov, M. Germann, Langmuir 20 (2004) 9913.
[32] A. Thormann, N. Teuscher, M. Pfannmöller, U. Rothe, A. Heilmann, Small 3 (2007) 1032.
[33] G.Q. Ding, M.J. Zheng, W.L. Xu, W.Z. Shen, Nanotechnology 16 (2005) 1285.